Giant magnetoresistance in Co-Cu-Ni granular ribbons

2000 J. Phys.: Condens. Matter 12 2525

(http://iopscience.iop.org/0953-8984/12/11/317)

J. Phys.: Condens. Matter **12** (2000) 2525–2533. Printed in the UK PII: S0953-8984(00)08019-X

Giant magnetoresistance in Co–Cu–Ni granular ribbons

F Wang†, T Zhao†, Z D Zhang†§, M G Wang†, D K Xiong†, X M Jin†, D Y Geng†, X G Zhao†, W Liu†, M H Yu† and F R de Boer ‡

† Institute of Metal Research and International Centre for Materials Physics, Academia Sinica, Shenyang 110015, People's Republic of China
‡ Van der Waals–Zeeman Institute, University of Amsterdam, Valckenierstraat 65, 1018XE, Amsterdam, The Netherlands

E-mail: zdzhang@imr.ac.cn

Received 21 September 1999, in final form 23 December 1999

Abstract. We have systematically investigated the structural, magnetic and transport properties of as-quenched and annealed $Co_{20}Ni_xCu_{80-x}$ ($0 \leqslant x \leqslant 20$) granular alloys prepared by melt spinning. The microstructure of granular ribbons of Co–Ni–Cu shows a matrix in which nanoparticles of Co–Ni are well distributed, very different from that of granular ribbons of Co–Cu in which full-grown Co microparticles are embedded in a Cu matrix. The phase segregation in the Co–Ni–Cu granular ribbons is not a pure nucleation and growth process as in the Co–Cu granular ribbons, but also not purely due to spinodal decomposition. In contrast to the ribbons with high Ni content, the low-Ni-content ribbons show an increase in magnetoresistance ($\Delta R/R \cong 6.2\%$ at 300 K for $Co_{20}Ni_5Cu_{75}$, which is larger than in as-quenched and annealed Co–Cu ribbons.

Since the discovery of giant magnetoresistance (GMR) in granular solids [1, 2] much attention has been paid to heterogeneous granular thin films. The electrical resistivity of heterogeneous granular Co–Cu [3], Co–Ni–Fe [4, 5], Co–Ag [6], Fe–Ag [7], Fe–Ni–Ag [8], Ni–Co–Ag [9], Co–Cu [10], Fe–Ni–Cu [11] and Fe–Co–Cu [12] thin films decreases with increasing magnetic field. It has become increasingly clear that the size distribution of the magnetic nanoparticles plays an important role in this phenomenon. It is widely accepted [3, 13] that the phase segregation in Co–Cu granular ribbons is a nucleation and growth process. It has been reported that the phase segregation of Co–Ni–Fe [4, 5] and Co–Ni–Cu [13] ribbons is spinodal decomposition. It also has been found that the MR amplitude decreases in the Co–Ni–Cu and Co–Ni–Fe granular ribbons, when these materials are cooled from room temperature to low temperature.

In the present paper, the GMR and the microstructure in $Co_{20}Ni_xCu_{80-x}$ ($x = 5$, 10, 15 and 20) granular ribbons prepared by melt spinning are reported. The phase segregation in the Co–Ni–Cu ribbons is not a pure nucleation decomposition or growth process. It is closely connected with the Ni content. In particular, in the Co–Ni–Cu granular ribbons with low Ni content, the magnetoresistance ratio is larger than in Co–Cu granular ribbons. In contrast to the ribbons with high Ni content [13], the low-Ni-content ribbons show an increase in magnetoresistance $\Delta R/R$ at low temperatures.

$Co_{20}Ni_xCu_{80-x}$ ribbons with $x = 2.5, 5, 7.5, 10, 15$ and 20 were prepared by melt spinning on a copper wheel in Ar atmosphere at wheel speeds of about 35 m s^{-1}. In order to maximize

§ Correspondence to Zhang Zhi-dong.

0953-8984/00/112525+09$30.00

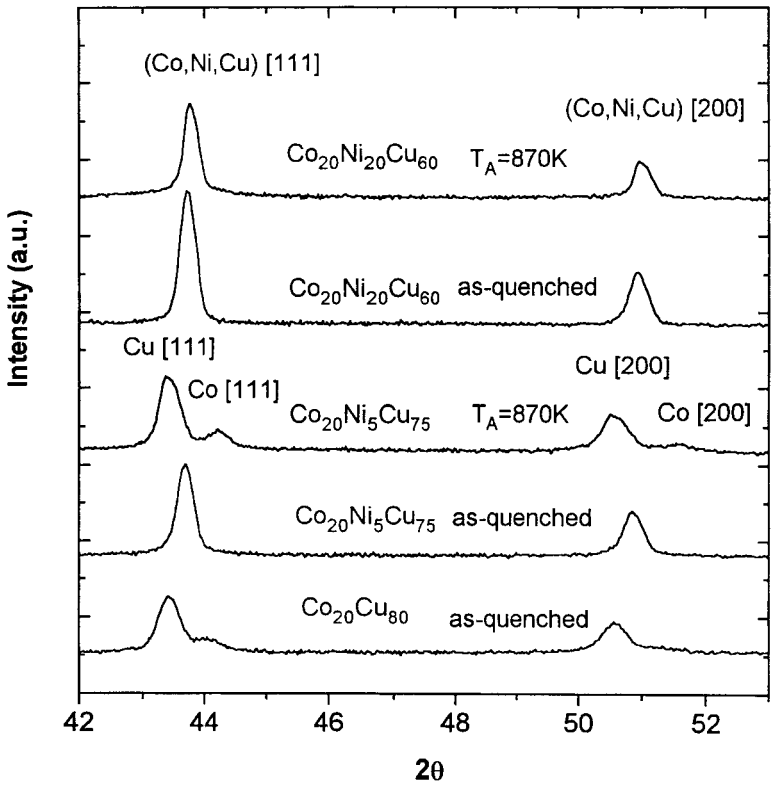

Figure 1. X-ray-diffraction patterns of as-quenched and annealed $Co_{20}Ni_xCu_{80-x}$ ($x = 0$, 5 and 20) ribbons.

the magnetoresistance, the prepared ribbons about 2 mm wide and 20 to 30 μm thick were annealed in the temperature range from 520 to 870 K. The electrical resistivity was measured by the standard dc four-terminal method. The magnetization was measured in the temperature range from 5 to 300 K and in magnetic fields up to 5 T, by using a superconducting quantum interference device (SQUID) magnetometer. The crystal structure was characterized by x-ray diffraction (XRD). The averaged chemical composition and the homogeneity of the ribbons were checked by means of a JSM-6301F scanning electron microscope (SEM) and an electron microprobe (EM). The microstructures of the ribbons were also studied by using a Philips FM420 analytic electron microscope (AEM) operated at 100 kV.

Figure 1 shows the XRD patterns of as-quenched $Co_{20}Ni_xCu_{80-x}$ ($x = 0$, 5 and 20) granular ribbons in the low-angle region. The peaks in the XRD pattern of as-quenched Co–Cu ribbons can be indexed to belong to the Co-rich and Cu-rich phases (the lowest curve in figure 1). As Ni is added, the peaks of the Co-rich phase are not observable in the as-quenched Co–Ni–Cu ribbons. The peaks of the Cu-rich phase are superposed by two sets of reflections, corresponding to two high-temperature (HT) phases $(Co(HT), Ni, Cu)_1$ and $(Co(HT), Ni, Cu)_2$. This observation is in agreement with the Co–Cu–Ni phase diagram as determined by Dannöhl and Neumann [14]. Upon introduction of Ni, the position of the peak of the Cu-rich phase moves slightly towards higher angle. After annealing at high temperatures for 10 min, the peaks corresponding to the Co-rich phase appear in the XRD pattern of the sample with 5 at.% Ni. The positions of peaks indicate the formation of the pure Co and pure Cu phases (the

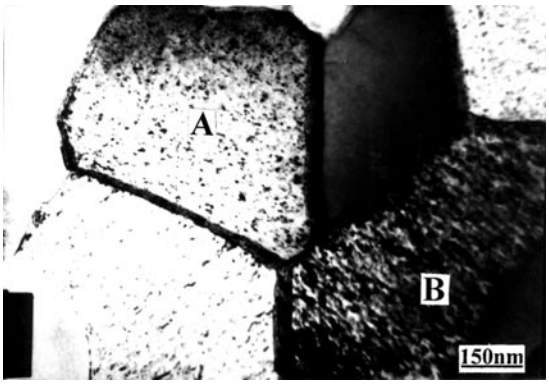

Figure 2. Bright-field transmission electron micrograph of as-melt-spun $Co_{20}Ni_5Cu_{75}$ ribbon after annealing for 10 min at 750 K.

middle curve in figure 1). This phenomenon, i.e. the phase separation, is not observable in the XRD pattern of the annealed 20 at.% Ni sample (the uppermost curve in figure 1). The positions of peaks shift to higher angles, indicating that the lattice parameter decreases with increasing Ni content.

The ribbons are polycrystalline with a grain size of about 100 to 500 nm, as determined by means of AEM and XRD. However, in the ribbons with low Ni content ($\leqslant$10 at.%), sometimes crystalline grains are observed in the very limited size range of 20 to 30 nm. Figure 2 shows the bright-field transmission electron micrographs of $Co_{20}Ni_5Cu_{75}$ ribbons annealed for 10 min at 750 K. As observed by AEM, there are two kinds of structure in the crystalline grains. One structure (denoted as A in figure 2) is of the granular alloy, in which Co particles of 2 to 3 nm are distributed the same as in the Co–Cu ribbons [15]. Another structure (represented as B in figure 2) is of the component-modulated type, which is a special feature of the Ni-containing ribbons. This type of structure is a direct result of the spinodal decomposition. However, depending on the Ni content, the situation is different in the various samples. In the as-quenched $Co_{20}Ni_5Cu_{75}$ ribbons, the component-modulated-structure profile is smeared out. Upon annealing, the component-modulated structure gradually forms in the low-Ni-content samples. After annealing for 10 min at 750 K, this kind of structure is very clearly observed by AEM (the diffraction patterns show splitting along the interface normal). In contrast to the $Co_{20}Ni_5Cu_{75}$ sample, the component-modulated structure is always clearly observable in both the as-quenched and the annealed $Co_{20}Ni_{20}Cu_{60}$. When the annealing temperature T_A is increased, the component-modulated structure is not clearly changed. It should be noted that a number of crystalline grains in the ribbons have this kind of structure so it may play an important role in GMR.

Figure 3 represents the zero-field-cooled (ZFC) and field-cooled (FC) (in a field of 0.01 T) magnetization curves of an as-quenched $Co_{20}Ni_5Cu_{75}$ ribbon. Below a characteristic freezing temperature, a large thermal hysteresis is observed (figure 3). The thermal hysteresis at temperatures far above the maximum of the ZFC curve indicates the existence of a broad distribution in size and shape of the magnetic precipitates. This suggests that the granular ribbon is a disordered magnetic system [3] that must have a rather complex magnetic behaviour. However, the situation of $Co_{20}Ni_5Cu_{75}$ ribbon is different from that of the Co–Cu ribbons, since the large Co-rich precipitates (20–50 nm) have disappeared (our experimental result for the Co–Cu ribbons is comparable to that reported in [15]), whereas the component-modulated structure has emerged.

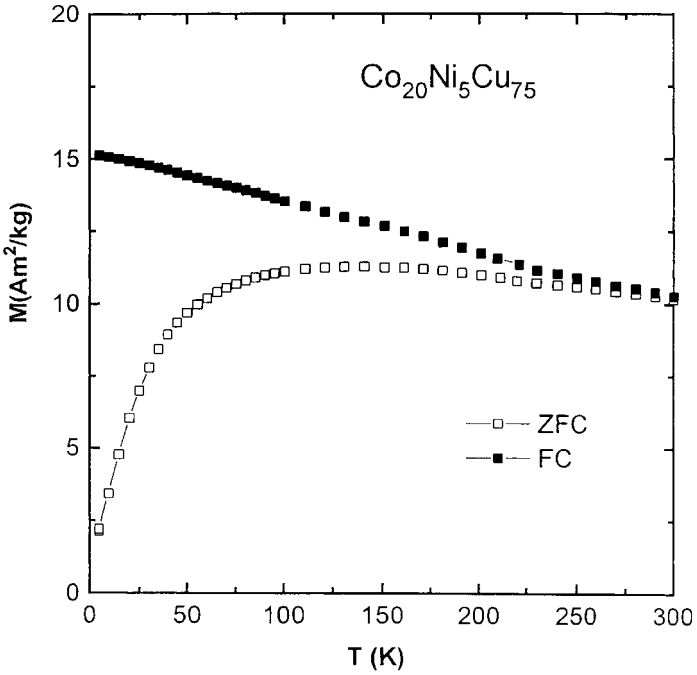

Figure 3. Zero-field-cooled and field-cooled ($B = 0.01$ T) magnetization curves for an as-melt-spun $Co_{20}Ni_5Cu_{75}$ ribbon.

Figure 4 shows the field dependence of the magnetoresistance MR ($=(R_H - R_0)/R_0$) ratio at room temperature for the samples with various Ni contents after annealing at 750 K for 10 min. When the Ni content increases, the MR amplitude decreases in good agreement with the results in Co–Ni–Cu multilayers [16] and sputtered [13] samples. It is found that $\Delta R/R$ of the $Co_{20}Ni_5Cu_{75}$ ribbons is larger than of the $Co_{20}Cu_{80}$ ribbons. The Co/Cu ribbons show an MR amplitude of 4.6% in 1.2 T, which is comparable to the value reported in [3]. However, the MR amplitude of $Co_{20}Ni_5Cu_{75}$ granular ribbon is found to be 6.2% in 1.2 T. This is the first time that an increase of the MR amplitude has been found by substitution of Ni for Cu and this result is completely different from that in the case of Co–Ni–Cu multilayers [16] or in sputtered granular films [13]. An explanation of this interesting result may be that the number of the magnetic CoNi-rich particles with smaller size (2–3 nm) increases in the Co–Ni–Cu granular ribbons, comparable to what happens in the Co–Cu granular ribbons. At the same time, the magnetic particles with larger size (20–50 nm) disappear. The formation of the small magnetic particles results in the formation of a large amount of interfaces, which is of benefit to the spin-dependent scattering of electrons. Furthermore, the component-modulated structure in the low-Ni-content samples may support the mechanism of the giant magnetoresistance as in magnetic multi-layers. Another explanation may be the reduction of the structural disorder in the Ni-containing ribbons after annealing at higher temperatures which leads to a decrease of the absolute resistivity in zero field. The dependence of the absolute resistivity change $\Delta\rho$ and the relative resistivity change $\Delta\rho/\rho$ exhibits peak behaviour.

Figure 5 shows the magnetoresistance at room temperature in a magnetic field of 1.2 T of melt-spun $Co_{20}Ni_xCu_{80-x}$ ribbons with $x = 5$, 10, 15 and 20 after annealing at different temperatures. It is found that, after annealing at various temperatures, the MR amplitude has

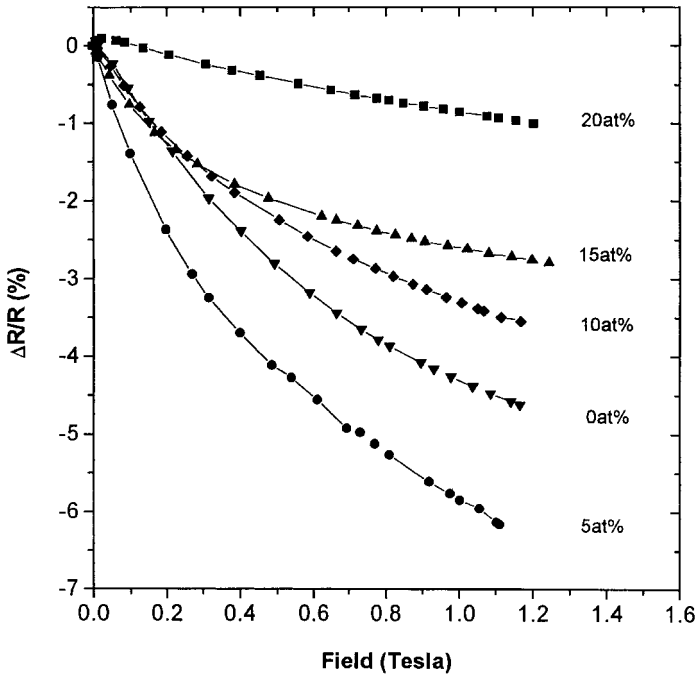

Figure 4. Magnetoresistance at room temperature of melt-spun $Co_{20}Ni_xCu_{80-x}$ ribbons with various Ni contents after annealing for 10 min at 750 K.

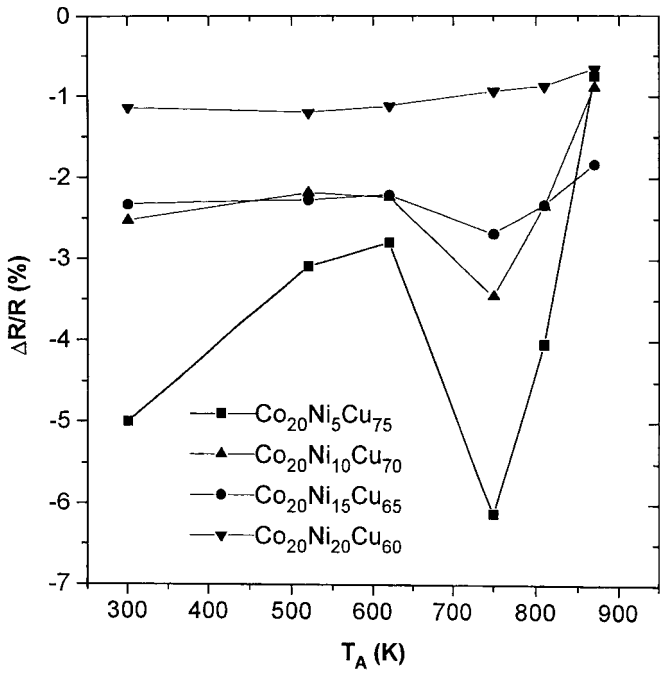

Figure 5. Dependence of the magnetoresistance at room temperature of melt-spun $Co_{20}Ni_xCu_{80-x}$ ribbons of various compositions on the annealing temperature T_A.

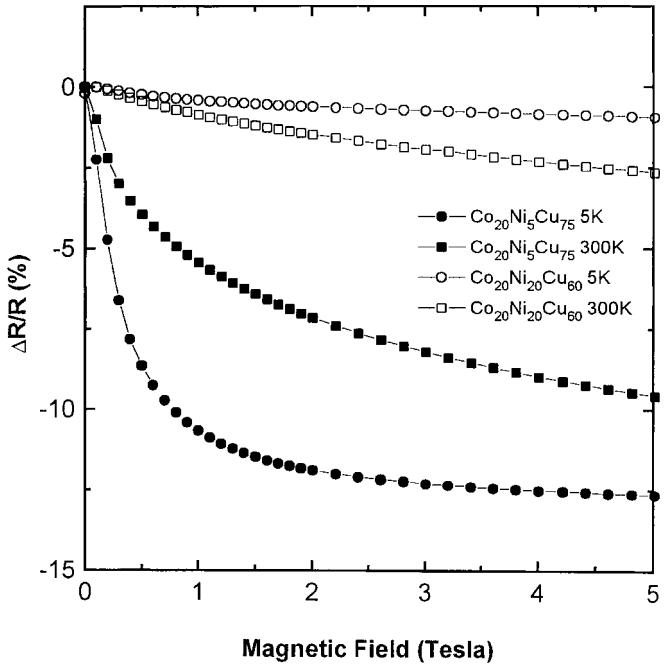

Figure 6. Magnetoresistance at 5 and 300 K of $Co_{20}Ni_5Cu_{75}$ and $Co_{20}Ni_{20}Cu_{60}$ granular ribbons after annealing for 10 min at 750 K.

the general tendency to decrease with increasing Ni content. For the $Co_{20}Ni_5Cu_{75}$ ribbon, the largest MR amplitude is obtained after annealing for 10 min at 750 K. The same annealing condition also leads to the largest MR amplitude for the samples with other Ni contents, with the exception of $Co_{20}Ni_{20}Cu_{60}$. The MR amplitudes in the $Co_{20}Ni_xCu_{80-x}$ ribbons with $x = 5$, 10 and 15 at first decrease when the annealing temperature is increased, then increase and at last decrease again. However, as can be seen in figure 5, the range of variation of the MR ratio becomes narrower with increasing Ni content in the ribbon. When the annealed temperature changes from 300 to 870 K, the range of the change of the MR ratio of the $Co_{20}Ni_5Cu_{75}$ ribbon is about 5%, whereas it is less than 1% for the $Co_{20}Ni_{20}Cu_{60}$ ribbon. This may be due to a change of the phase segregation in the Co–Ni–Cu granular ribbon from a nucleation and growth process to pure spinodal decomposition, upon increasing Ni content.

Figure 6 shows the MR ratio at 5 and 300 K as a function of the applied magnetic field for $Co_{20}Ni_5Cu_{75}$ granular ribbon annealed for 10 min at 750 K. With increasing magnetic field, the electrical resistivity of the ribbon decreases monotonically. The ribbon with 5 at.% Ni exhibits a negative room temperature magnetoresistance ratio of about 9.5% at $B = 5$ T. The MR amplitude at 5 K of the same sample is 12.6%. This is in contrast with the $Co_{20}Ni_{20}Cu_{60}$ granular ribbon, annealed under the same conditions, of which the MR amplitudes are 2.6% and 0.9% at 300 and 5 K, respectively. So, although the ribbons with 5 and 20 at.% Ni both exhibit two kinds of structure of the crystalline grains, the temperature dependence of the MR is opposite for the two samples. The MR ratio shows a tendency to saturate with increasing magnetic field, in particular at 5 K.

Figure 7 represents magnetization curves at room temperature of as-quenched $Co_{20}Ni_xCu_{80-x}$ ($x = 0$, 2.5, 5 and 7.5) granular ribbons. When the Ni content increases

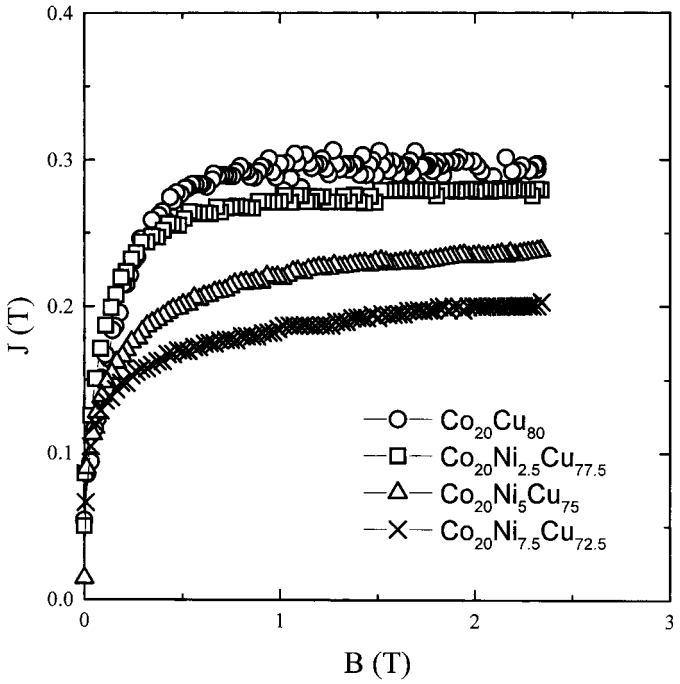

Figure 7. Magnetization curves at room temperature of as-quenched $Co_{20}Ni_xCu_{80-x}$ ($x = 0$, 2.5, 5 and 7.5) granular ribbons.

from 0 to 7.5 at.%, the saturation magnetization decreases. This is because during rapid quenching, the formation of CoNiCu solid solutions decreases the content of the magnetic CoNi-rich phases. Since the CuNi phase is non-magnetic, the magnetization of CoNiCu solid solutions should be lower than that of the CoNi phases. Figure 8 shows magnetization curves at room temperature of $Co_{20}Ni_5Cu_{75}$ and $Co_{20}Ni_{20}Cu_{60}$ granular ribbons after annealing for 10 min at different temperatures. Annealing at temperature above 620 K increases rapidly the saturation magnetization of as-quenched $Co_{20}Ni_5Cu_{75}$ granular ribbons. However, the saturation magnetization remains nearly unchanged for annealing at 620–870 K because the further annealing only results in the growth of the magnetic particles. On the other hand, the saturation magnetization of $Co_{20}Ni_{20}Cu_{60}$ granular ribbons depend sensitively on the annealing temperature T_A, which is ascribed to the spinodal decomposition.

In summary, we report the giant magnetoresistance in granular CoCuNi ribbons. We find that the phase segregation in the CoCuNi granular ribbons is connected with the presence of Ni. There are two kinds of structure in the crystalline grains. The component-modulated structure gradually forms after annealing in the low-Ni-content ribbon, but has not been found in multilayer and sputtered samples. The largest GMR is found for a ribbon with composition $Co_{20}Ni_5Cu_{75}$, annealed for 10 min at 750 K. At room temperature in a field of 1.2 T, the MR amplitude of this ribbon exceeds 6%, which is larger than what is found under the same conditions for Co–Cu. The granular ribbons with low Ni contents show an MR amplitude which increases as the temperature is lowered, which is opposite to the ribbons with high Ni content. The experimental results imply that the microstructure plays an important role in the Co–Ni–Cu ribbons and that the component-modulated structure may strongly contribute to the GMR.

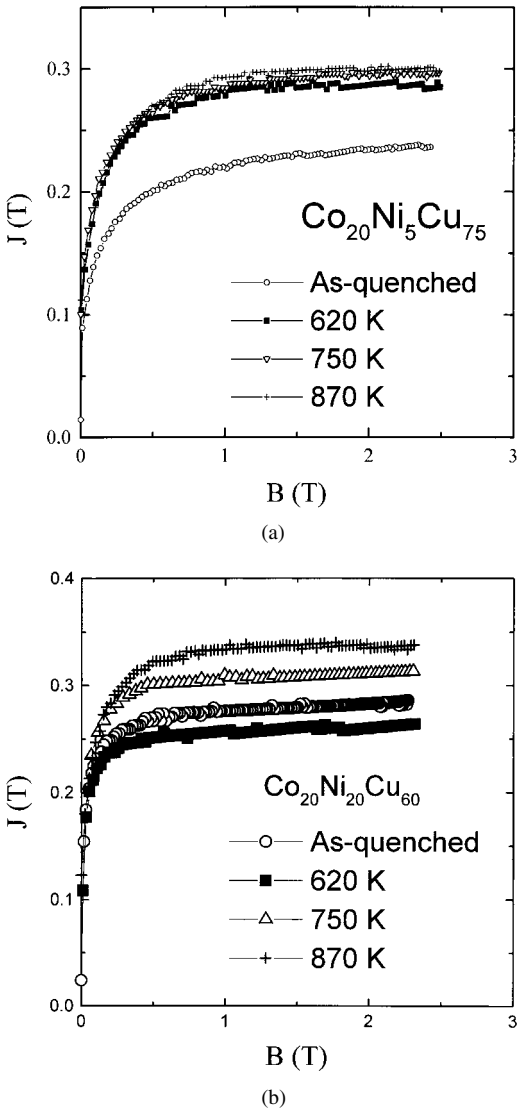

Figure 8. Magnetization curves at room temperature of (a) $Co_{20}Ni_5Cu_{75}$ and (b) $Co_{20}Ni_{20}Cu_{60}$ granular ribbons after annealing for 10 min at different temperatures. The values for annealing temperature T_A are shown in the figure.

Acknowledgments

We thank the National Natural Sciences Foundation of China for the support of the projects No 59725103, 59831010 and 59871054 and the Sciences and Technology Commissions of Shenyang and Liaoning. This work has been carried out within the scientific exchange programme between China and the Netherlands.

References

[1] Berkowitz A E, Mitchell J R, Carey M J, Young A P, Zhang S, Spada F E, Parker F T, Hutten A and Thomas G 1992 *Phys. Rev. Lett.* **68** 3745

[2] Xiao J Q, Jiang J S and Chien C L 1992 *Phys. Rev. Lett.* **68** 3749

[3] Dieny B, Chamberod A, Cowache C, Genin J B, Teixeira S R, Ferre R and Barbara B 1994 *J. Magn. Magn. Mater.* **135** 191

[4] Jin S, Chen L H, Tiefel T H, Eibschutz M and Ramesh R 1994 *J. Appl. Phys.* **75** 6915

[5] Chen L H, Jin S, Tiefel T H and Wu T C 1994 *J. Appl. Phys.* **76** 6814

[6] Xiong P, Xiao G, Wang J Q, Xiao J Q, Jiang J S and Chien C L1992 *Phys. Rev. Lett.* **69** 3220

[7] Tsoukatos A, Wan H, Hadjipanayis G C, Unruh K M and Li Z G 1993 *J. Appl. Phys.* **73** 5509

[8] Jiang J S, Xiao J Q and Chien C L 1992 *Appl. Phys. Lett.* **61** 2362

[9] Kitada M, Yamamoto K and Shimizu N 1993 *J. Magn. Magn. Mater.* **124** 243

[10] Wecker J, Helmolt R V, Schultz L and Samwer K 1993 *Appl. Phys. Lett.* **62** 1985

[11] Martins C S, Rechenberg H R and Missell F P 1998 *J. Appl. Phys.* **83** 7001

[12] Rubinstein M, Harris V G, Das B N and Koon N C 1994 *Phys. Rev.* B **50** 12 550

[13] Zhang S Y and Cao Q Q 1996 *J. Appl. Phys.* **70** 6261

[14] Dannöhl W and Neumann H 1943 *Z. Metallk.* **22** 1

[15] Wang W D, Zu F W, Weng J, Shao J M and Lai W Y 1997 *J. Chin. Electron Microsc. Soc.* **16** 290

[16] Kano H, Iwasaki Y, Hayashi K and Aso K 1993 *J. Magn. Magn. Mater.* **126** 445